

6. V. I. Zalkind et al., "Magnetohydrodynamic method of obtaining electrical energy," in: Collection of Articles [in Russian] (edited by V. A. Kirillin and A. E. Sheindlin), No. 3, *Énergiya*, Moscow (1972), p. 84.
7. V. S. Chirkin, *Thermophysical Properties of Materials of Nuclear Technology* [in Russian], Atomizdat (1968).

THERMAL-SHOCK PERFORMANCE OF EVAPORATED  
 $Al_2O_3$ ,  $ZrO_2$ , AND LAMINATED CERMET  
 COATINGS IN AN ELECTRIC-ARC PLASMA SOURCE

V. S. Leshchenko, V. G. Novikov,  
 A. V. Petrov, A. D. Sukhobokov,  
 and E. A. Turkin

UDC 533.6.071.1:62-69.  
 629.78.023.222

Measurements have been made on the thermal stability and performance of protective coatings deposited by plasma-gun techniques on copper with an arc heater.

The working materials in an arc heater are subject to very severe stress, the main causes of failure being thermal shock, erosion, surface reactions, and embrittlement [1]. Protective coatings can provide reliable operation at high temperatures, since they restrict oxidation, improve the stability under erosion, and provide control over the heat transfer to the circulating coolant by conduction.

The performance of such a coating is dependent on the rates of heat transfer and the nature of the substrate. At present, we have no coatings that can be used at all the temperatures that occur in such heaters, but such coatings are of value even at moderate temperatures, since they ease the strain on the working materials, optimize the cooling conditions, and reduce the heat loss.

The coatings most widely used are  $Al_2O_3$  and  $ZrO_2$ ; these are stable in oxidizing atmospheres and have high melting points ( $\sim 2300^\circ K$ ), while their thermal conductivities are relatively low,  $0.5 < \lambda < 4$ , and industrial techniques are available for deposition [2].

The working gas parameters in such heaters are  $1000 < T_0 < 5000^\circ K$  and  $P_0 > 50 \cdot 10^5 N/m^2$ , and the heat loss through the discharge chamber increases with the pressure, and so the components have to be protected from high heat fluxes; also, the continuous working time is such that a steady-state temperature distribution is usually set up.

This steady state is reached in a short time, and therefore a thermal shock occurs on switching the device on; naturally, the coating material must be resistant to such shocks.

The deposition technique must ensure good adhesion to the substrate; if the bond is poor, the coating may fail for mechanical or thermal reasons, and also on account of differences in linear expansion coefficients.

TABLE 1. Deposition Conditions

Material	Nozzle diameter, mm	Gas flow, liters/sec		Gas used to supply powder	Current, A	Voltage, V	Distance from end of nozzle to workpiece, mm
		Ar	H <sub>2</sub>				
$Al_2O_3$	5-7	30-60	6-8	3-6	350	60	100-130
$ZrO_2$		40-50	4-5		460	60-75	100-120
NA-67		30-50	6-8		350	60	200-250

Translated from *Inzhenerno-Fizicheskii Zhurnal*, Vol. 31, No. 3, pp. 443-448, September, 1976.  
 Original article submitted July 23, 1975.

*This material is protected by copyright registered in the name of Plenum Publishing Corporation, 227 West 17th Street, New York, N.Y. 10011. No part of this publication may be reproduced, stored in a retrieval system, or transmitted, in any form or by any means, electronic, mechanical, photocopying, microfilming, recording or otherwise, without written permission of the publisher. A copy of this article is available from the publisher for \$7.50.*

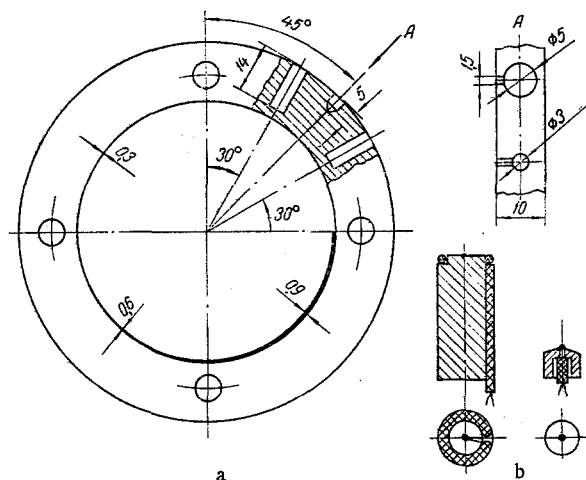


Fig. 1. Ring with heat-resistant coating: a) positions of thermocouples; b) method of mounting thermocouples.

Therefore, it is of some interest to test the performance of coatings of oxide type under working conditions. Such tests should involve coatings of various thicknesses, although excessive thicknesses are hazardous from the viewpoint of internal stress and also adversely affect the cooling of the coating itself, which may mean that the surface melts in contact with the hot gas. Naturally, the stability under shock loading must be examined and for a variety of loads. It is also desirable to test the resistance and performance not only of coatings currently in use, but also of new materials, particularly when the base material is copper. It is difficult to discuss the performance of a coating from the purely theoretical viewpoint on account of the numerous factors that influence the performance deposition technique, temperature dependence of the thermophysical characteristics, and so on.

Here we report measurements on the performance and viability of coatings deposited by plasma methods:  $\text{Al}_2\text{O}_3$ ,  $\text{ZrO}_2$ , and  $\text{Al}_2\text{O}_3 + \text{Mo}$ , each of these on copper; the thicknesses were varied, and also the heat-flux densities. By performance of such a coating one means the reduction in the heat flux through the wall produced by the coating in comparison with the uncoated material under the same conditions.

### Apparatus and Methods

Experiments were done with a coaxial discharge system similar to that described in [3]; the temperatures and the heat-loss distributions were measured on the outer electrode (cathode), and the diameter of the central electrode (anode) was 55 mm, with the internal and external diameters of the cathode 80 and 114 mm, respectively. The outer electrode was sectioned, and it took the form of a cylindrical bush assembled from

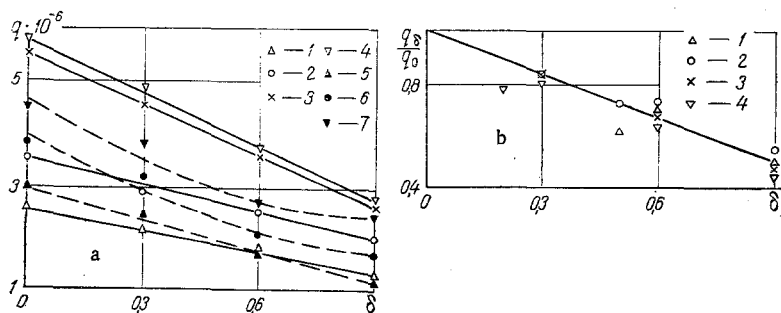


Fig. 2. Distribution of heat flux in wall in relation to coating thickness for  $G = 7 \cdot 10^{-3} \text{ kg/sec}$  and  $P_0 = 6 \cdot 10^5 \text{ N/m}^2$ : a) distribution of heat flux density: 1)  $N = 0.106 \text{ MW}$ ; 2)  $0.136$ ; 3)  $0.186$ ; 4)  $0.209$ ; 5)  $0.125$ ; 6)  $0.140$ ; 7)  $0.194$ ; solid lines  $\text{Al}_2\text{O}_3$ ; broken lines  $\text{ZrO}_2$ ; b) relative change in heat loss:  $q$ ,  $\text{W/m}^2$ ;  $\delta$ , mm.

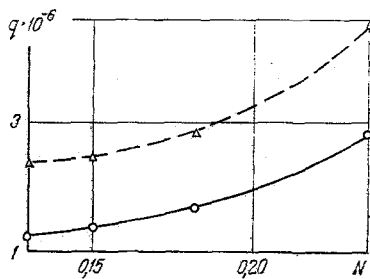


Fig. 3. Distribution of heat-flux density in wall in relation to electrical power for  $G = 7 \cdot 10^{-3}$  kg/sec,  $P_0 = 6 \cdot 10^5$  N/m<sup>2</sup>, Al<sub>2</sub>O<sub>3</sub> + Mo. Solid line)  $q_\delta$ ; broken line)  $q_0$ ;  $q$ , W/m<sup>2</sup>;  $N$ , MW.

copper rings, with a ring of width 30 mm in the discharge zone, but rings of 10 mm elsewhere. The sectional outer electrode had a standard gap between each of the rings, which eliminated any heat leak along the electrode itself, and thus measurement of the temperature distribution gave a reliable indication of the local heat flux averaged over the width of a ring. Also, this sectioned outer electrode provided a simple means of testing rings with various protective coatings. A ring bearing a coating was placed directly in the discharge zone. The position of the coated ring was constant in the various sets, so constant values for  $I$ ,  $U$ , and  $P$  produced similar temperatures in the region of the ring. Each such ring was uncoated over one quarter of the perimeter, while the other three quadrants were coated each with a different thickness.

The measurements were made with Chromel—Copel thermocouples of wire diameter 0.3 mm; Fig. 1 shows the scheme used in measuring the temperatures and also the disposition of the thermocouples. Each sector contained three thermocouples: one in the middle at a distance of 5 mm from the outer edge and two at distances of 3.0 mm from the inner edge. In the case of couples near the hot surface, holes of diameter 5 mm were drilled to the required depth, the bottom end of a hole being flat. In this a plug was fitted, with the thermocouple wire inside it; the junction was attached to the center, and the leads were brought out via a slot in the side. When the plug had been inserted, the upper end was sealed with K-300 cement. When the couples were set near the cooling channels, the bushing was made in a different style: diameter 3.0 mm, conical end, height 2.5 mm. The thermocouple wire was inserted through a central hole and fixed in place with cement. Identical heat-transfer conditions were provided by sealing the wires as described above, and making similar sealed holes in adjacent rings, but without fitting thermocouples. In addition, the wires were brought out through rubber seals in the side arms.

Measurements were made of the following: wall temperature in the ring, gas flow rate through the heater, chamber pressure, and  $I$  and  $U$  in the discharge. The parameters were measured with N-010 oscillographs. The coefficient of variation for the results, which included the error in installing the thermocouples, the error of the recording equipment, and the error in interpreting the oscillograms, was about  $\pm 8\%$ .

The measurements were made in air with a flow rate of  $G = 7 \cdot 10^{-3}$  kg/sec, total pressure  $P_0 = 6 \cdot 10^5$  N/m<sup>2</sup>, gas temperature at the exit  $3000 < T_0 < 4500$ , and discharge current  $400 < I < 1000$  A. Each ring was tested in 15 heat loading cycles each of duration about 20 sec.

The coatings were deposited on the rings by means of a UPU-3M commercial equipment for plasma deposition of refractory materials, which was developed by the Automated Technology Scientific-Research Institute. We used zirconium dioxide grade 4MTU-8-18-68 of grain size 28-40  $\mu\text{m}$ , and also GA85 aluminum oxide, GA8-GOST 6912-64, grain size 40-100  $\mu\text{m}$ . The underlayer was of NA-67 thermally reactive material. Table 1 gives the deposition conditions. The metal—ceramic coatings were based on ZrO<sub>2</sub> + Co and Al<sub>2</sub>O<sub>3</sub> + Mo, and the latter material was also tested in the electric-arc heater.

## Results

The performance was evaluated from the heat loss through the part protected by the coating, which was compared with the loss through the uncoated part. The temperature distribution was deduced from the part of the recording where the values remained unchanged, i. e., on the assumption that a one-dimensional steady state had been attained. Figure 2 shows the results for various input powers  $0.1 < N < 0.22$  MW; the variation of the heat loss through the wall with the coating thickness ( $\delta = 0.3, 0.6, \text{ and } 0.9$  mm) was linear. In the case

of  $ZrO_2$  films, this no longer applied at high heat fluxes and for thick coatings, which was due to destruction of the surface layer (sintering), because the thermal conductivity of  $ZrO_2$  at high temperatures is much less than that of  $Al_2O_3$ . The relative reduction in the heat loss was almost constant for a given coating thickness as the power input was varied. Two types of coating (alumina and zirconium dioxide) were comparable in performance, the heat flux for the largest thickness,  $\delta = 0.9$  mm, being about 40-50% of that for an unprotected ring. At the smallest coating thickness, the reduction in the heat loss was only 15-20%. Visual examination showed that the aluminum oxide worked reliably in this range of heat fluxes and thicknesses. There was no cracking or detachment of the  $Al_2O_3$  layer. The  $ZrO_2$  coatings were less effective. For instance,  $\delta = 0.5$  mm resulted in cracks, while  $\delta = 0.9$  mm caused the coating to flake off after several loading cycles. Tests were made on rings with  $Al_2O_3$  coatings of thicknesses 0.2, 0.5, and 0.9 mm. The heat losses for these cases agreed well with those shown in Fig. 2b.

The fluctuations in flow rate in the cooling system and variations in nozzle setting meant that we could not provide identical heat losses in a ring together with identical volt-ampere characteristics. However, the metal-ceramic coatings of thicknesses 0.2, 0.5, and 0.9 mm worked reliably, as no cracks or flaking was seen. The effective thermal conductivity of such a coating was dependent on the number of layers. For instance, the effective thermal conductivity at first increases with the number of layers, which is probably due to the contribution of the metallic component, with only a slight effect from the contact resistances. The effective thermal conductivity fell as the number of layers increased further, although it still remained higher than that for the ceramic base material. The resistance of the metal-ceramic coatings to thermal shock was due to the metal phase acting as a damper. The layers of metal embedded in the ceramic improved the performance by reducing the differences in linear expansion between the various materials. Figure 3 shows the heat-flux distribution for a metal-ceramic coating of thickness  $\delta = 0.2$  mm; a mixed coating is clearly more effective than the pure ceramic.

#### NOTATION

$T_0$ , temperature, °K;  $q$ , heat flux density,  $W/m^2$ ;  $\lambda$ , thermal conductivity,  $W/m \cdot deg$ ;  $P_0$ , gas pressure,  $N/m^2$ ;  $G$ , gas flow rate,  $kg/sec$ ;  $I$ , current, A;  $U$ , voltage, V;  $N$ , electrical power, MW;  $\delta$ , thickness of thermal protective layer, mm.

#### LITERATURE CITED

1. J. Huminik, Jr. (editor), High-Temperature Inorganic Coatings [Russian translation], Metallurgiya, Moscow (1968).
2. V. S. Leshchenko, Yu. T. Nikitin, and L. S. Gushchina, Nauchn.-Issled. Inst. Avtomat. Tekhnol. Ser. 4, No. 337 (1973).
3. A. D. Sukhobokov, E. A. Turkin, S. V. Shalaev, and G. I. Shcherbakov, Inzh.-Fiz. Zh., 26, No. 1 (1974).